Multi-material additive manufacturing of steels using laser powder bed fusion

Nadimpalli, Venkata Karthik; Dahmen, Thomas; Valente, Emilie Hørdum; Mohanty, Sankhya; Pedersen, David Bue

Published in:
Proceedings of the 19th International Conference and Exhibition (EUSPEN 2019)

Publication date:
2019

Document Version
Publisher's PDF, also known as Version of record

euspen's 19th International Conference & Exhibition, Bilbao, ES, June 2019
www.euspen.eu

Multi-material additive manufacturing of steels using laser powder bed fusion

Venkata Karthik Nadimpalli[1], Thomas Dahmen[1], Emilie Hørdum Valente[1], Sankhya Mohanty[1], David Bue Pedersen[1]

[1] *Technical University of Denmark, Department of Mechanical Engineering, 2800 Kgs. Lyngby, Denmark*

vkna@mek.dtu.dk

Abstract

Most commercially available laser powder bed fusion (L-PBF) systems are limited to process one material at a time. The ability to spatially apply multiple materials within the same component will strongly expand the available design space for engineers. A typical problem with multi-material components is stress concentration at discrete material interfaces. Functionally graded interfaces could be used to overcome this limitation. In this work, an open-architecture L-PBF system from Aurora Labs was used to mix and process stainless steel 316L and maraging steel MS1 powder. Thereby, continuous and discrete interfaces between both materials were generated and characterized regarding microstructure, micro-hardness, and elemental composition. An L-PBF process window was found to gradually change the composition of 316L to MS1 creating a continuous interface. The controlled mixing of the powders in each layer indicates the versatility of the powder dispensation setup for multi-material combinations. This contribution will further pave the way towards the development of functionally graded L-PBF components.

Metal additive manufacturing, multi-material, functionally graded components, adaptive process control, MS1, 316L

1. Introduction

The possibility to apply multiple materials within one component further expands the large design space provided by additive manufacturing processes. So far, directed energy deposition processes (DED) are mainly associated with multi-material additive manufacturing in metals due to their intrinsic system-related flexibility of changing to different feedstocks during operation. However, powder-bed fusion (PBF) based additive manufacturing processes exhibit specific advantages over DED such as the possibility to generate more intricate geometries and achieving smaller feature sizes. At the same time, most commercially available PBF systems are limited to a single powder feedstock restricting the deployment of different materials during the build process [1].

Four different levels of multi-material PBF can be observed in literature as summarized in table 1. Every PBF system is capable of level one multi-material management by printing on top of either different build plate materials or on top of existing geometries with a different material (I). Examples of such applications are found in [2-3]. Level two multi-material management pre-requisites the capacity to change the feedstock material during the process (II). In doing so, machine modifications such as additional powder hoppers or powder containers with separate compartments are necessary [4-9].

However, to avoid stress concentrations at the discrete interface of two materials, a more gradual transition is realized by level three multi-material management (III). For instance, Demir and Previtali introduced a prototype L-PBF system with two powder feeders in combination with piezoelectric transducers for in-situ gradual mixing of Fe and Al-12Si powder [10]. While level three multi-material management can be characterized through the specific control of material composition in one direction, level four enables full spatial control in all directions (IV). This capability has been demonstrated by Wei et al. custom made L-PBF system with multiple powder feeders and a point-by-point micro-vacuum selective material removing system [11].

The different materials being investigated differ in most mechanical properties such as tensile strength, yield strength, modulus of elasticity, tangent modulus, etc. as well as in thermal properties such as specific heat capacity, conductivity, melting temperatures , and latent heat. One highly relevant property for PBF, however, is the mismatch in thermal expansion coefficient for the two materials which naturally give rise to high stresses at the interfaces for (I) and (II). Continuous transitioning of materials in (III) and (IV) would reduce the thermal mismatch and lead to better stress states within functionally graded components.

In this work, multi-material cuboids in stainless steel 316L and maraging steel MS1 ranging from level one to three were built with an open-architecture L-PBF system and subsequently investigated. This material system was chosen because of the high strength of MS1 and the corrosion resistance in combination with the wide availability of 316L which makes it ideal for numerous applications.

Table 1 Prior contributions of multi-material PBF in metals with regard to the achieved level of spatial material control, resulting interfaces, and placement of this work

Level	***I***	***II***	***III***	***IV***
Spatial resolution	2D 	2D 	2D 	3D 
Interface	discrete	discrete	continuous	continuous
Sources	[2 – 3]	[4 – 9]	[10]	[11]
	Scope of present work			

2. Methodology

Two multi-material cuboids were generated combining 316L with MS1 material on three different levels. On the first level, cuboids (10x10x7mm) were manufactured in MS1 on top of a 316L build plate (I). At the second level, cuboids were generated in MS1 on top of printed 316L cuboids on top of a 316L build plate (II). Here, the feedstock material was abruptly changed at the interface between the 316L and MS1 cuboid. The third level multi-material experiment involved a gradual change between both materials at the interface of one cuboid (III). A schematic overview of the three set-ups is provided in figure 1.

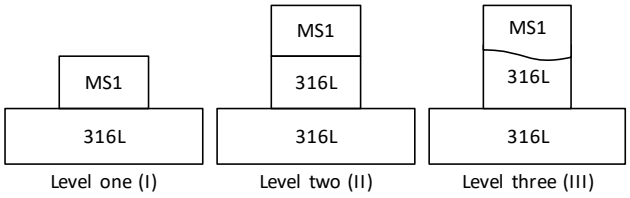

Figure 1. Additively manufactured multi-material cuboids

2.1. Experimental set-up

In the following, the two different feedstock materials that are used in this paper are introduced. Thereafter, the machine set-up to simultaneously process multiple materials is presented.

AISI 316L stainless steel powder from LPW technology was used with a particle size of 53 ± 15 µm. The build plates were made out of the identical material. The second feedstock material, MaragingSteel MS1, was provided by EOS GmbH. The particle size is specified as > 63 µm according to ASTM B214. The specifications for the chemical composition of both materials are shown in table 2.

Table 2 AISI 316L SS and EOS MaragingSteel MS1 powder, chemical composition in wt. %

	316L powder												
	Fe	**C**	**Si**	**Mn**	**Cr**	**Ni**	**Mo**	**Cu**	**N**	**O**	**Ti**	**Al**	**Co**
min	-	-	-	-	17.5	12.5	2.25	-	-	-	-	-	-
max	bal	0.03	0.75	2	18	13	2.5	0.5	0.1	0.1	-	-	-
	MS1 powder												
	Fe	**C**	**Si**	**Mn**	**Cr**	**Ni**	**Mo**	**Cu**	**N**	**O**	**Ti**	**Al**	**Co**
min	-	-	-	-	-	17	4.5	-	-	-	0.6	0.05	8.5
max	bal	0.03	0.1	0.1	0.5	19	5.2	0.5	-	-	0.8	0.15	9.5

The two materials were processed by an Aurora Labs S-Titanium Pro laser powder bed fusion (L-PBF) system, which combines two 150 W CO_2-laser sources simultaneously. The two beams pass separately through a set of optics before entering into the focus lens resulting in a single spot with approx. 150 µm in diameter in the processing plane. Thereby, the focus lens is mounted onto a moving print head in an X-Y gantry system as shown in figure 2. The average maximum power output of the focused beam is 255 W and was measured with a Gentec-EO 300 W power meter at the processing plane.

In comparison to other L-PBF processes, the Aurora Labs system is unique in its powder dispensation as it uses a set of individual powder hoppers located above the build chamber. Dosed amounts of powder are supplied through a controlled rotation of an extrusion screw positioned at the exit of each hopper. Thereby, the powder is fluidized and transported by the inert gas supply of the system through a set of interconnected tubes to the print head.

During the process, the powder dispensation in each layer is based on two steps. In the first step, the powder is dispensed onto the machine bed by a continuous linear x-movement of the print head across the width of the build plate. In the second step, a sweeping mechanism spreads the deposited powder across the build plate in y-direction resulting in one homogenous layer of powder. The relatively long path of transport through the tubes (~300 mm) in combination with the powder dispensation and the sweeping mechanism ensure thorough mixing of the materials.

The open-architectural design of the system allows the user to fully access and modify the G-code that the machine is operating on. Thus, all process parameters can be defined line-by-line.

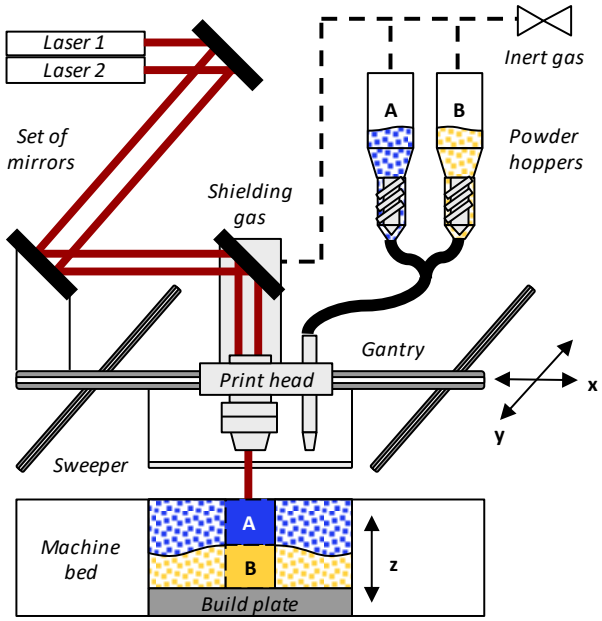

Figure 2. Used machine set-up for multi-material L-PBF

The process parameters that are kept constant across all builds are given in table 3.

Table 3 Used process parameters of builds

Parameter	**Value**
Laser power, P_L	255 W
Wavelength of CO_2 lasers, λ_{CO2}	10600 nm
Scan speed, v_{scan}	30-40 mm/s
Spot diameter, d_{spot}	150 µm
Hatch distance, d_{hatch}	120 µm
Layer thickness, d_{layer}	30 µm
Scan track rotation between layers, α	90°
Build plate temperature, T_{build}	90 °C
Powder hopper temperature, T_{hopper}	50 °C
Oxygen level in build chamber	<0,1 %

The scan speed v_{scan} of the moving print head is adapted based on the respective material. Prior to this study, process parameters for 316L and MS1 were individually studied and optimized. Figure 3 shows the polished and etched cross-section of an MS1 component built on the present L-PBF system. Process parameters were optimized until the porosity was reduced significantly. A typical L-PBF microstructure was observed with long columnar grains. The clear visibility of the grains in the microstructure was due to the 90° rotated scan strategy. Process optimization was also performed for 316L builds on 316L build plates beforehand [12]. Hence, for processing 316L v_{scan} was set to 40 mm/s and v_{scan} = 30 mm/s for MS1.

Figure 3. Panoramic stiched light optical microscope image of processed MS1 powder on the Aurora Labs L-PBF system

Creating level two and three multi-material cuboids were realized by manually changing the G-code. Thereby, the amount of powder drawn from each hopper can be specified within each layer. For the level two cuboids, the feedstock and scan speed was exchanged from 316L to MS1 in the mid-layer of the G-code (II). For the level three cuboids, the weight percentage of mixing within each layer was specified. Figure 4 shows the applied mixing ratio of dispensed powder in the gradual interface (III). In addition to this, the scan speed in the interface region (Layer 80 – 114 and 1.05 mm in height) is gradually adapted in three steps from 40 mm/s to 30 mm/s.

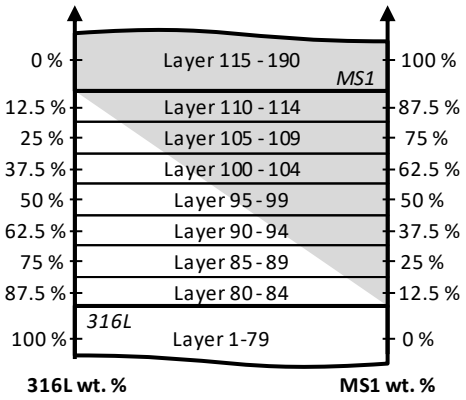

Figure 4. Schematic of gradual level three (III) transition from 316L to MS1 among layers with a thickness of 30 µm

2.2. Materials characterization

The samples were cut using a slow speed saw, embedded and polished until 4000 grit SiC paper followed by 3 µm and 1 µm diamond paste. One set of samples was used for microhardness while the other one was etched using Kallings Reagent No.1 by swabbing for two seconds followed by rinsing. Any longer etch period led to better etching on 316L but over etched the MS1 parts. The microstructure of the etched cross-sections was investigated by light optical microscopy (LOM, Zeiss Axio A1).

Hardness tests were conducted on a FutureTech FM-700 Vickers microhardness tester with a 100 g load and 10 s load time. The tests were conducted on the XZ cross-section along the building height, always transitioning from SS 316L into MS1. Five line scans were performed on each sample to get an average and standard deviation for the microhardness values.

The interface between L-PBF 316L and MS1 was investigated by scanning electron microscopy (SEM, Gemina Supra 35, Carl Zeiss) using energy-dispersive x-ray spectroscopy (EDS, ThermoFisher Scientific), on cut cross-sections, ground and polished as the embedded samples, followed by OPS polishing.

3. Results and discussion

3.1. Structure and properties

Vickers microhardness tests on three levels of multi-material L-PBF components are shown in figure 5. In level one and level two multi-material cuboids, the discrete nature of the interface was evident from the hardness values. An abrupt change in hardness from one material to the other is visible with a transition zone around 100 µm on either side. The similar behaviour in (I) and (II) interfaces is expected since a sudden change in material causes a discrete interface.

In the level three interface, a statistically significant gradual change in hardness was observed. The transition region was designed to be 1 mm from one material to the other and the hardness values clearly indicate that the in-situ mixing of materials was well distributed. On average, the weight percentage of each material was a good indicator of the expected hardness values.

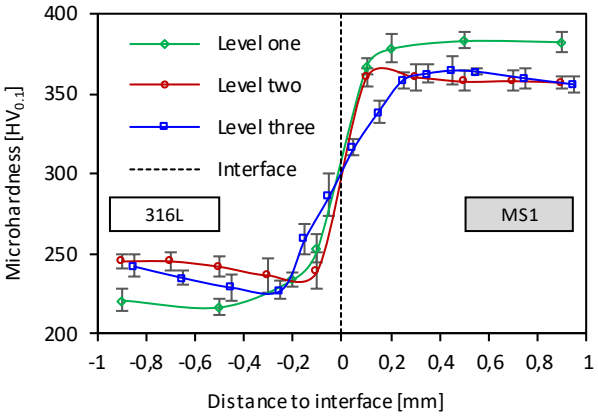

Figure 5. Vickers microhardness profiles around the interface for three levels of L-PBF multi-material components

The microstructure of level two and three material interfaces were investigated. Figure 6 shows the LOM images taken at and around the interface. The MS1 material was more sensitive to the etchant in comparison to 316L. Hence the contrast in the microstructure showed a gradual change from one material to the other. The increasing quantity of MS1 along the continuous interface led to the better visibility of the scan tracks and microstructural features.

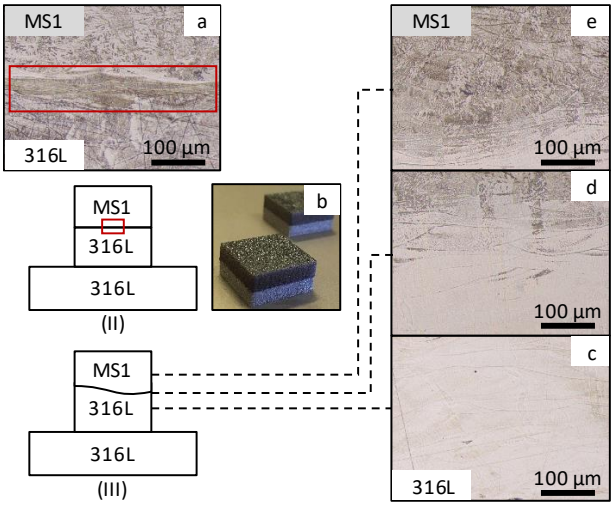

Figure 6. Schematic of level two and level three interfaces indicating the location of micrographs, a-b) level two discrete interface, c-e) gradual transition from 316L to MS1 in level three interface

3.2. Elemental composition

Elemental mapping was used to characterize the different types of multi-material interfaces. By this procedure, the chemical composition of the area under consideration can be studied with ~1 µm resolution. The elements of interest are Fe, Ni, Cr, Co, Mn, Mo, etc.. Chromium has a higher concentration in SS 316L, while, Iron, Nickel, Cobalt, and Molybdenum are higher in MS1.

Figure 7 shows the elemental map of the two interfaces which represents a qualitative comparison of the discrete (II) vs. the continuous (III) interface. The transition of Cr in the discrete interface is starkly contrasted with the transition in the continuous interface where a smooth and gradual change was observed. The samples presented in this work have some large porosities due to a deterioration of the focus lens by the time of manufacturing. However, as previously shown in figure three, high density can be achieved in MS1 components.

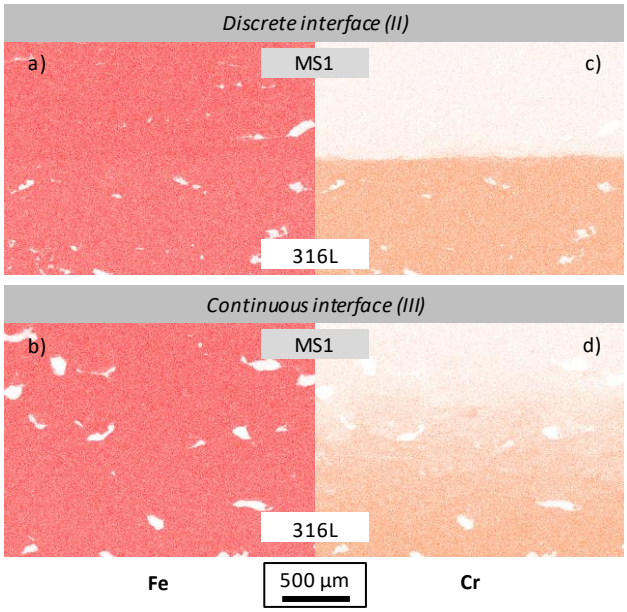

Figure 7. SEM-EDS elemental maps of Iron (a,b) and Chromium (c,d) in level two and level three interfaces respectively.

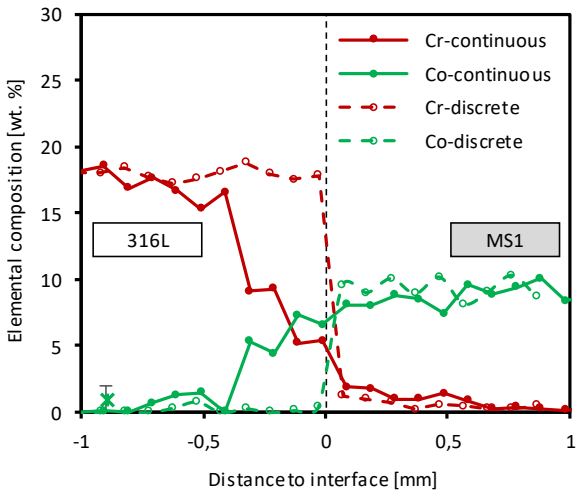

Figure 8. SEM-EDS line scans representing the wt. % of Cobalt and Chromium around the interface for discrete (level two) and continuous (level three) multi-material components

To quantify the difference across the interface an EDS line scan showing the changing concentration (wt. %) of Cr and Co is shown in figure 8. Elemental maps of Ni, Mn, Mo also showed similar trends. Around 0.5 mm from the interface on the 316L side, the decrease in Cr and increase in Co begin at the same time. From here, they gradually change as the amount of MS1 increases until 0.5 mm after the interface region. The gradual change observed from the elemental maps, confirmed by the EDS line scans, microhardness and microstructure indicate that the in-situ mixing and the adaptive process control in the defined region were successful.

4. Conclusions and future work

Multi-material processing in L-PBF is a relatively less explored area primarily due to the closed architecture of commercially available systems that are designed for processing one material at a time. Four levels of multi-material processing were defined based on the spatial control of deploying material in L-PBF. In this work, an Aurora Labs S-Titanium Pro L-PBF system was used to conduct three multi-material experiments with different steel powders. Thereby, 316L and maraging steel MS1 powder were mixed and processed on three different levels.

On level one, maraging steel MS1 cuboids were printed on top of 316L build plates. On level two, MS1 cuboids were printed on top of 316L printed cuboids. In addition to this, a level three multi-material experiment was conducted including a gradual transition in the interface of both materials. The resulting discrete interfaces (level one and two) and continuous interfaces (level three) were studied in terms of microstructure, micro-hardness, and elemental composition.

An L-PBF process window has been found to gradually change the composition of 316L to MS1 in a controlled manner without visible crack formation. The continuously changing interface can reduce the stress concentration present in a discrete interface. The controlled in-situ adaptive mixing of the powders in each layer showcases the advantage of the powder-drop setup for multi-material processing. In comparison to level four point-to-point drop methods which give a three-dimensional spatial control, level three methods are a suitable compromise in terms of processing speed and applicability to current L-PBF systems.

A primary challenge to be addressed in sophisticated multi-material processes (level two to four) is the subsequent separation of unfused mixed powders. However, the potential advantages of multi-material processing can justify the additional related costs. In the future, various other material combinations can be explored for microstructural design and manufacturing of functionally graded components.

References

[1] Bandyopadhyay A and Heer B 2018 *Materials Science & Engineering R* **129** 1-16

[2] Fox P, Pogson S, Sutcliffe C J and Jones E 2008 *Surface & Coatings Technol.* **202** 5001-5007

[3] Hinojos A, Mireles J, Reichardt A, Frigola P, Hosemann P, Murr L E and Wicker R B 2016 *Materials and Design* **94** 17/24

[4] Regenfuß P, Streek A, Hartwig S, Klötzer S, Brabant T, Horn M, Ebert R and Exner H 2007 *Rapid Prototyping Journal* **13** 4 204-212

[5] Terrazas C A, Gaytan S M, Rodriguez E, Espalin D, Murr L E, Medina F and Wicker R B 2013 *Int. J. Adv. Manuf. Technol.* **71** 33-45

[6] Liu Z H, Zhang D Q, Sing S L, Chua C K and Loh L E 2014 *Materials Characterization* **94** 116-125

[7] Sing S L, Lam L P, Zhang D Q, Liu Z H and Chua C K 2015 *Materials Characterization* **107** 220-227

[8] Guo C, Ge W and Lin F 2015 *Engineering* **1** 1 124-130

[9] Demir A G and Previtali B 2017 *Manufacturing Letters* **11** 8-11

[10] Beal V E, Erasenthiran P, Hopkinson N, Dickens P and Ahrens C H 2006 *Int. J. Adv. Manuf. Technol.* **30** 844-852

[11] Wei C, Li L, Zhang X and Chueh Y 2018 *CIRP Annals Manufacturing Technology* **67** 245-248

[12] Valente E H, Nadimpalli V K, Andersen S A, Christiansen T L, Pedersen D B, Somers M A J 2019 *Euspen Int. Conf. & Exh.* **19**